JOURNAL OF MATERIALS SCIENCE (1977) 1361–1375

Low-temperature TSD measurements on γ-irradiated polyvinylidene fluoride

A. CALLENS
Rijksuniversitair Centrum, Antwerpen, Belgium

L. EERSELS, R. DE BATIST*
Materials Science Department, S.C.K./C.E.N., B-2400 Mol, Belgium

As a part of the fundamental study of the relaxational behaviour of the semi-crystalline polymer polyvinylidene fluoride ($-(CH_2-CF_2)_n-$, PVDF), thermally stimulated depolarization (TSD) measurements have been carried out on γ-irradiated thin films, poled *in vacuo*. Following irradiation, the total TSD relaxation strength below room temperature is depressed. Mathematical analysis of this region of the TSD spectrum reveals the reduction to be caused by the decrease of the β-(glass-transition) relaxation peak. One also observes the irradiation-induced creation of two relaxation peaks, both with higher activation energies than their neighbours. Tentative interpretations for the different components of the relaxation spectrum are proposed.

1. Introduction

Thermally stimulated depolarization (TSD) has been recognized as a powerful tool for studying the discharging of polymer electrets [1–4] and in particular for the study of the post-irradiation behaviour of these materials [5–9]. Boyer, in his critical review [10] on glassy transitions in semi-crystalline polymers, has pointed out that because of its low equivalent frequency (sometimes lower than 10^{-3} Hz), TSD can be more successful in resolving close-lying relaxation processes than the more conventional dielectric and mechanical techniques. According to Boyer, a polymer material having about 50% crystallinity should be a favourable subject to test the above assumption. Our material meets this requirement. The dielectric and mechanical relaxation behaviour of unirradiated PVDF has been extensively studied by conventional methods (see [11] and references mentioned there). TSD has been used on several occasions for the relaxation study of unirradiated material, both for its fundamental aspects [12–15] and in research directed towards applications of the pyro- and piezo-electric properties of PVDF [16–19].

Electret discharging in semi-crystalline polymers is caused mainly by reorientation of polar chain segments and by Maxwell–Wagner proccesses at the crystalline–amorphous interfaces. As pointed out by Van Turnhout [3], dipolar TSD occurs predominantly in the lower temperature part of the TSD spectrum, which is the one treated in this paper. In a forthcoming paper, we propose to discuss the higher temperature zone (above 270 K), which can probably be ascribed to Maxwell–Wagner effects.

2. The material

For the present TSD study of the semi-crystalline polymer PVDF commercial thin films have been used, which were prepared and graciously put at our disposal by Solvay (Brussels). By X-ray Laue spectroscopy, following Gal'perin's method [20], these films were found to be of the mixed ($\alpha + \beta$) type and the degree of crystallinity about 44%. This is somewhat lower than the degree of crystallinity determined on bulk specimens of the same origin by X-ray spectroscopy and density measurements [11].

* Also at: Rijksuniversitair Centrum, Antwerpen, Belgium.

3. Irradiation and post-irradiation characterization

γ-irradiation has been carried out at ambient temperature either in a ^{60}Co source of the "Instituut voor Radio-Elementen (IRE)" at Mol or by means of spent fuel elements from the BR2 reactor. The ^{60}Co set-up yielded a dose rate of 240 krad h^{-1} and the fluence was limited to 100 Mrad. The BR2 fuel element cells give a dose rate of ~ 5 Mrad h^{-1}, allowing one to reach 1000 Mrad in about 1 week. The specimens were placed in pyrex tubes, either evacuated ($\sim 10^{-5}$ Torr) or in an air. Specimens, irradiated in air with doses higher than 50 Mrad are completely embrittled and of no use for further TSD investigation. Suwa *et al.* [21] observed similar effects in γ- or electron-irradiated PVDF films of trade mark KUREHA and attributed them to oxidative degradation. The experimental results reported here only refer to the samples irradiated *in vacuo*. Characterization has been performed by different techniques such as differential thermal analysis (DTA), X-ray Laue spectroscopy and infrared spectroscopy.

By DTA on bulk material, a decrease in the crystalline melting temperature T_M has been observed (from 454 K at zero dose to 408 K at 400 Mrad). According to Flory [22, 23], this can be related to a change in crystallinity:

$$\frac{1}{T_M} - \frac{1}{T_{M,0}} = -\frac{R}{\Delta H_f} \ln X$$

where T_M and $T_{M,0}$ are the crystalline melting temperature after and before irradiation, R is the universal gas constant, ΔH_f is the fusion enthalpy of the crystallites, which in first approximation has been considered as a constant (~ 1.4 kcal mol^{-1} [24]), and X is the crystalline mole fraction after irradiation relative to $X = 1$ before irradiation. Thus one can estimate a decrease in the degree of crystallinity between 0 and 400 Mrad from 44% to 28%.

The degree of crystallinity χ, can also be determined from the Laue spectra by:

$$\chi = \frac{I_{tot} - I_a}{I_{tot}},$$

where I_a and I_{tot} stand for the intensities of the lines as determined from their surface. The amorphous background I_a has been determined by Gal'perin's method [20], the total surface I_{tot} by planimeter. Using this method, one finds a change in crystallinity between 0 and 400 Mrad from 44% to 34%.

Infra-red spectroscopy reveals a pronounced increase with dose of the intensity of several lines in the 1600 to 1900 cm^{-1} region. This group of lines can be related [25–27] to double-bond stretching vibrations, e.g. $CH_2 = CHF$ (1654 cm^{-1}), $CF_2 = CH_2$ (1723 cm^{-1}) and other compounds listed in [25].

The interpretation of the spectra in this wave number region is rather ambiguous, however, due to the possible occurrence of several lines which are typical for the presence of the fluorinated carbonyl group, e.g. $-CF_2CH_2-COF$ (1730 cm^{-1}), and others listed in [25]. Suwa *et al.* [28] even attribute the total increase in intensity to this carbonyl group. It is also possible that oxydation caused by oxygen absorbed at the surface is responsible for part of the increase in intensity.

Complementary to the characterization techniques mentioned above, tensile tests on plate-shaped bulk material reveal a sharp increase in yield stress and initial modulus in the early stages of irradiation (0 to 50 Mrad), followed by a steady but slight decrease. These phenomena are typical for the post-irradiation behaviour of semi-crystalline polymers [29], the steep increase in the material strength being due to rapidly saturing cross-linking and the subsequent slow depression being due to a steady loss of crystallinity, as observed by DTA and X-ray spectroscopy. This is consistent with literature data, based mainly on solubility measurements [30, 31].

4. Thermally stimulated depolarization of dipolar polymer electrets

Van Turnhout [3] has reviewed the processes responsible for the fundamental transitions in polymeric materials, as detected by TSD. As has been mentioned already, two important groups of relaxations may occur in a semi-crystalline polymer such as PVDF: at low temperatures, mainly dipolar effects occur, whilst above the glass transition, interface effects are predominant. Dipolar reorientation is caused by the polarity of the $(-CH_2-CF_2-)$ chain segment and accompanies changes in the mobility of the main chain backbone. Interface (Maxwell–Wagner) polarization occurs at the boundary between regions with different dielectric constant and different specific conductivity, e.g. at

the interface between crystalline and amorphous regions in semi-crystalline polymers. Because, analytically, it is not possible to decide whether a relaxation is of dipolar or Maxwell–Wagner origin [32–34], physical treatments are required to do so (heat, irradiation, mechanical deformation, etc). The results reported here are restricted to the low temperature region ($T < 300$ K). The method used for analysing dipolar relaxation is, therefore, briefly outlined below, based on the general development given in [3].

When a polymer electret, formed by poling at a temperature between the glass transition and the crystalline melting temperatures, is allowed to depolarize at a temperature well below the glass transition, the polarization P is given by:

$$\frac{dP}{dt} + \frac{1}{\tau(T)} P = \frac{\epsilon_0(\epsilon_s - \epsilon_\infty)}{\tau(T)} E_p, \qquad (1)$$

where E_p is the poling field, $\tau(T)$ the temperature-dependent relaxation time, ϵ_0 the dielectric constant *in vacuo*, ϵ_s and ϵ_∞ the relative dielectric constants at low and at high frequencies respectively. For polymers, the saturation value of the relaxation strength $(\epsilon_s - \epsilon_\infty)$ can be approximated by a formula based on the Langevin expression:

$$(\epsilon_s - \epsilon_\infty) \simeq \frac{N\mu^2}{3\epsilon_0 k T_p}, \qquad (1a)$$

where N is the number of polar monomer units per unit volume, μ their dipole moment, k the Boltzmann constant, T_p the poling temperature (in K). With the boundary condition $P(t_0) = 0$ (t_0 being an arbitrary starting time):

$$P(t) = \epsilon_0(\epsilon_s - \epsilon_\infty)E_p \left\{1 - \exp\left[-\int_{t_0}^{t} \frac{dt'}{\tau(T')}\right]\right\} \qquad (2)$$

The depolarization current is given by:

$$j(t) = \frac{dP}{dt} = \frac{\epsilon_0(\epsilon_s - \epsilon_\infty)}{\tau(T)} E_p \exp\left[-\int_{t_0}^{t} \frac{dt'}{\tau(T')}\right]. \qquad (3)$$

Integration of Equation 3 is simplified, if one applies a linear heating rate ($\beta = dT/dt$):

$$j(T) = \frac{\epsilon_0(\epsilon_s - \epsilon_\infty)}{\tau(T)} E_p \exp\left[-\frac{1}{\beta}\int_{T_0}^{T} \frac{dT'}{\tau(T')} .\right] \qquad (3a)$$

The temperature dependence of the relaxation time $\tau(T)$ is not necessarily of the Arrhenius form. The integral in Equation 3a, however, is considerably simplified if an Arrhenius-like dependence is used, with non-distributed parameters τ_0 and $E[\tau(T) = \tau_0 \exp(E/kT)]$. E then represents either the true activation energy, if the process is really Arrhenius-like, or the apparent activation energy, if it is either of another type or highly distributed.

Equation 3a finally becomes:

$$j(T) = \frac{N\mu^2 E_p}{3\tau_0 k T_p} \exp\left[-E/kT - \frac{1}{\beta\tau_0}\int_{T_0}^{T} \exp(-E/kT')dT'\right]. \qquad (3b)$$

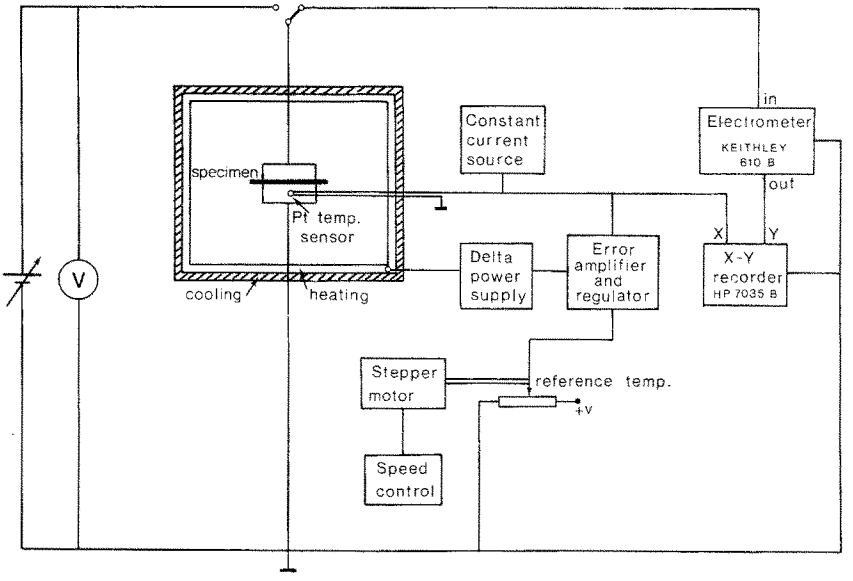

Figure 1 Schematic diagram of the TSD apparatus. The polymer film is fixed between two electrode blocks. Resistive linear heating is programmed at rates between 0.1 and 9.9 K min^{-1}. Cooling is achieved by means of a liquid nitrogen flow in the container wall. Potential difference over the Pt resistance thermometer and the TSD current constitute the X and Y co-ordinates for the X–Y recorder.

It should be borne in mind that for semi-crystalline polymers, which are rather complex in nature, Equation 3b may only be used as a rough approximation. The apparent activation energy E can only be meaningfully compared with results obtained using the same method. True values of E can, of course, be determined by the peak shift method in dynamic mechanical and dielectric experiments, carried out at different frequencies.

5. Experimental equipment for TSD measurements

As can be deduced from the short theoretical treatment above, the temperature is an important factor in the design of TSD equipment. Gradients over the specimen should be avoided and the heating rate is to be kept constant. A schematic technical description of the equipment is given in Fig. 1.

To allow a direct comparison between the TSD

TABLE I Standard poling characteristics

Specimen thickness	20 μm
Poling field	12.5 MV m^{-1}
Poling potential	250 V
Poling temperature	353 K
Poling time	30 min
Cooling rate	not constant in about 1 h from ~350 K to ~150 K
Heating rate	1 K min^{-1}

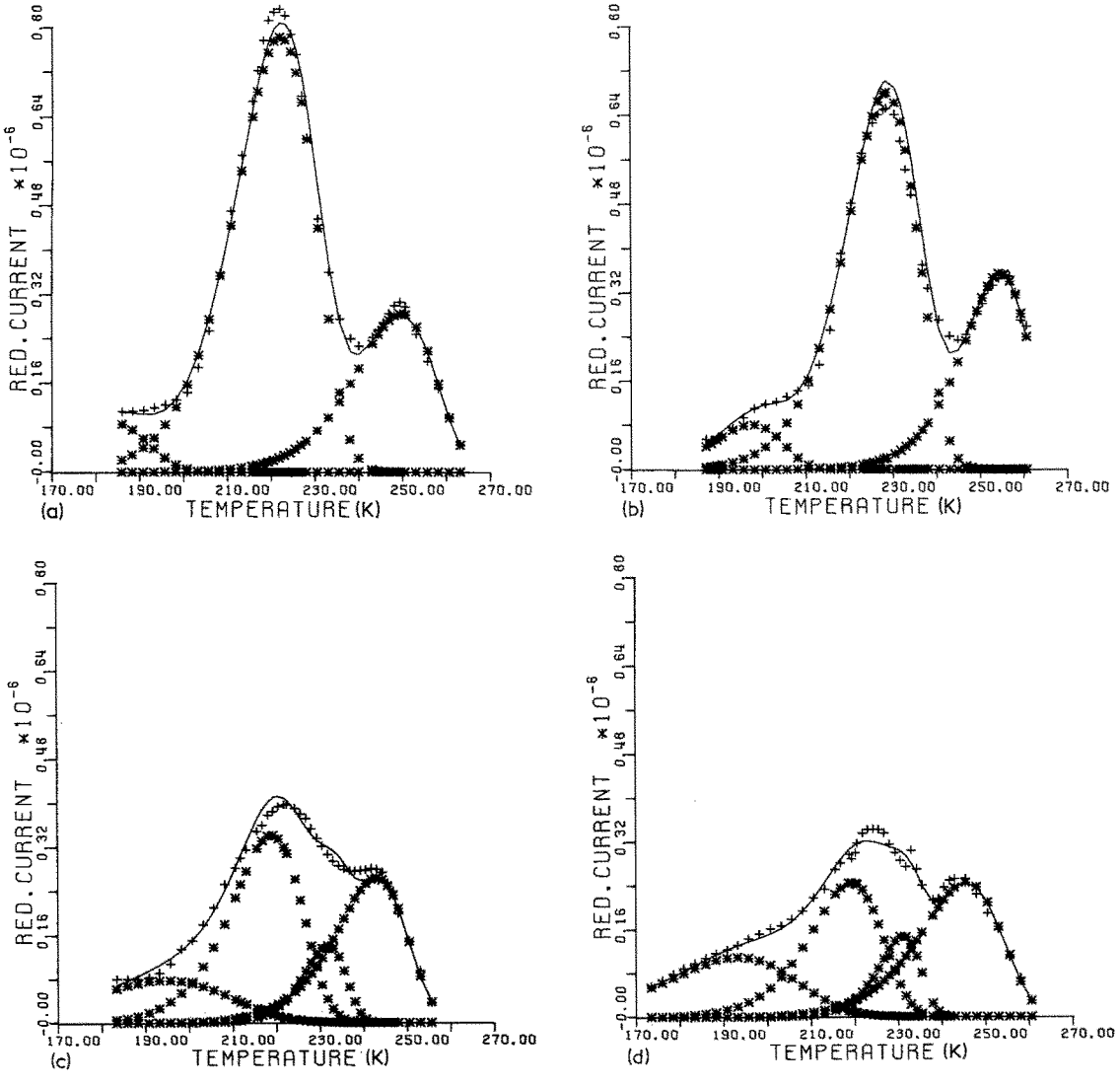

Figure 2 Low-temperature TSD spectra corresponding to γ-irradiation doses of: ^{60}Co: 0(a), 5(b), 50(c), 100(d) Mrad, and BR2: 100(e), 200(f), 300(g), 400(h) Mrad. The experimental current values are given by +, the current contributions of the various components by *, and the sum of the fitted components by a continuous line. The curves corresponding to the "BR2" dose range, are shown at enlarged scale.

spectra at different irradiation doses, poling and current measuring conditions have been standardized. They are given in Table I.

To eliminate experimental scatter, TSD runs on a specimen have been performed at least twice and sometimes measurements on different specimens with the same history have been done.

6. Experimental results and analysis

TSD spectra for temperatures below room temperature, corresponding to γ-irradiation doses of 0, 5, 50, 100 (^{60}Co), 100, 200, 300, 400 Mrad (BR2 fuel element cells), are shown in Fig. 2a to h. A drastic decrease in the total below room temperature relaxation strength with irradiation dose is obvious. The depression is steep for the low dose region ($\leqslant$20 Mrad) and continues steadily up to higher doses. An analogous depression is observed in the mechanical relaxation strengths measured by internal friction (Fig. 3) [35].

Matveev *et al.* [36] have obtained a more gradual decrease in the relaxation strength by conventional dielectric measurements. The temperature range where those effects occur suggests that they are mainly caused by morphological changes in the amorphous phase [11]. Therefore it is possible to analyse the spectra in terms of Equation 3b. The experimental depolarization current, j_{tot}, may be

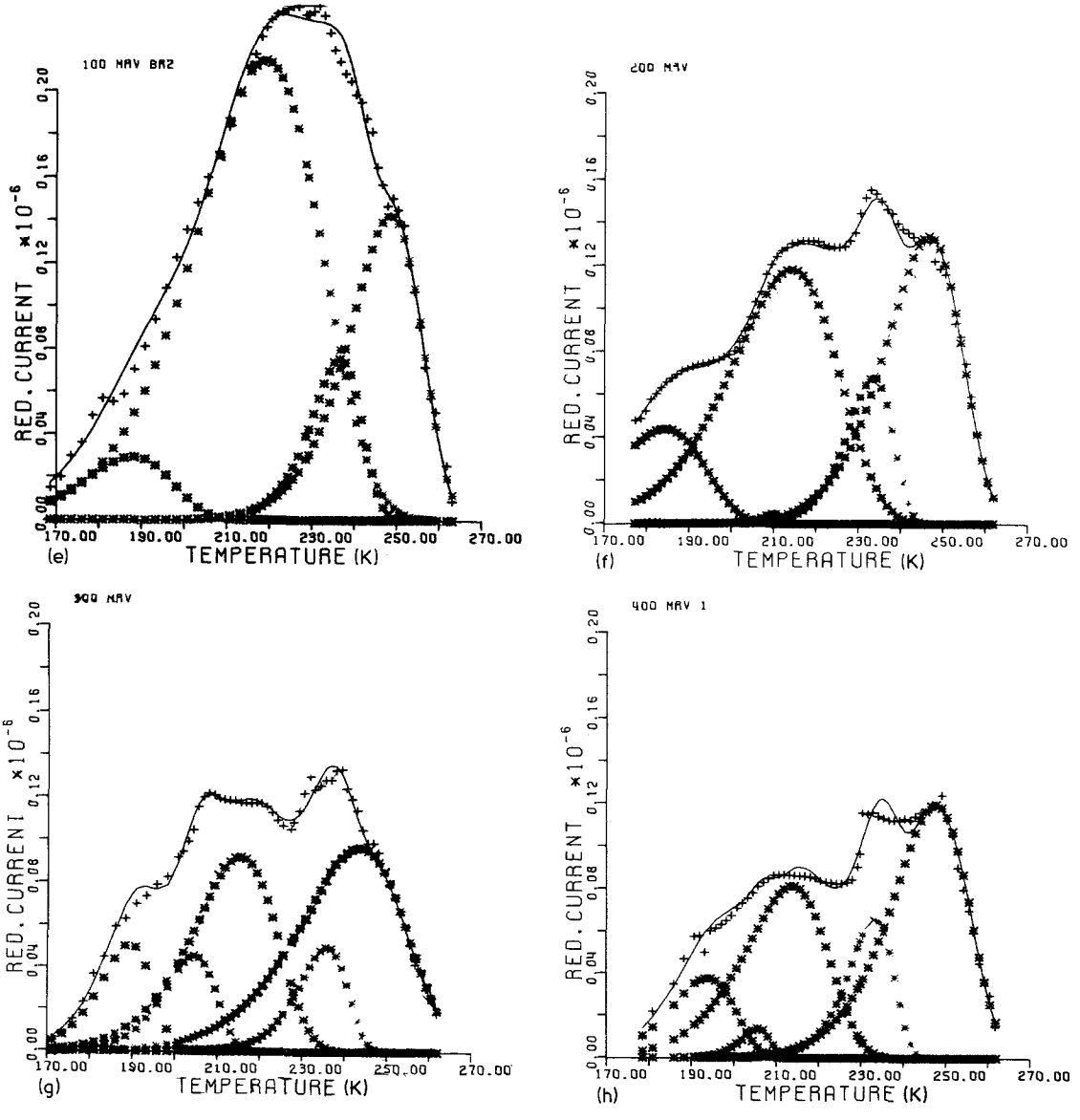

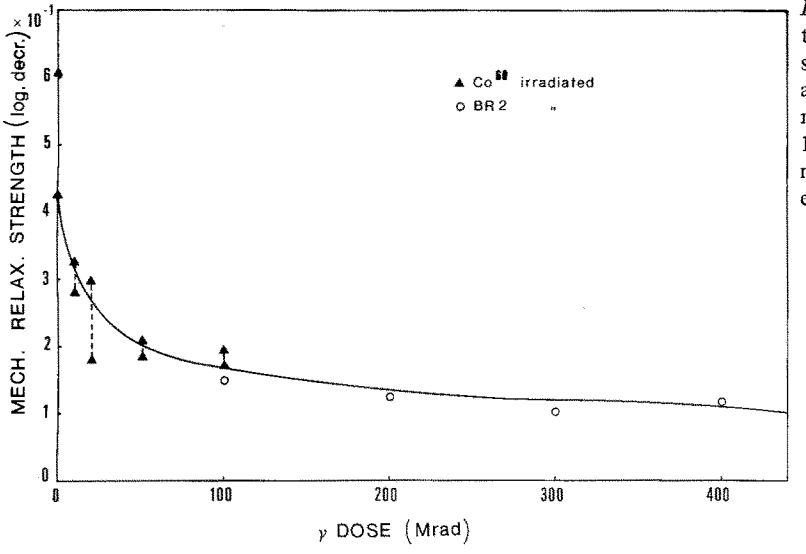

Figure 3 Dependence on dose of the total mechanical relaxation strength of the β relaxation region as measured by a flexural resonance method (frequency about 100 Hz) on platelet PVDF specimens. The dotted lines connect extreme experimental results.

decomposed in a number, N, of current contributions $j_i(T)$ of type (Equation 3b):

$$j_{tot}(T) = \sum_{i=1}^{N} j_i(T)$$

$$= \sum_{i=1}^{N} \frac{N_i \mu_i^2 E_p}{3kT_p \tau_{o,i}} \exp\left[-\frac{E_i}{kT} - \frac{1}{\beta\tau_{o,i}} \int_{T_0}^{T} \exp\left(\frac{E_i}{kT'}\right) dT'\right]. \quad (4)$$

Because Equation 4 is impractical for mathematical manipulation, Cowell and Woods [37] have developed an approximate expression. The reliability of their approximation has been successfully tested by several authors [38, 12].

According to Cowell and Woods' approximation, and using reduced units ($j = j_{exp}/\epsilon_o E_p$), Equation 4 becomes;

$$j_{tot} = \sum_{i=1}^{N} j_i(T) \simeq \sum_{i=1}^{N} A_i \exp[-t_i - B_i t_i^{-2} \exp(-t_i)] \quad (4a)$$

where

$$t_i = E_i/kT, \quad (4a')$$

$$A_i = \frac{N_i \mu_i^2}{3\epsilon_o k T_p \tau_{o,i}}, \quad (4a'')$$

and

$$B_i = E_i/k\beta\tau_{o,i}. \quad (4a''')$$

Estimates for A_i and B_i to be used in Equation 4a may be derived from the experimental values $t_{i,m}$, $j_{i,m}$ and $T_{i,m}$, corresponding to the peak current:

$$t_{i,m} = E_{i,m}/kT_{i,m} \quad (4b)$$

$$A_i \simeq j_{i,m} \exp\left(\frac{t_{i,m}^2 + 3t_{i,m}}{t_{i,m} + 2}\right) \quad (4c)$$

$$B_i \simeq \exp(t_{i,m}) \left(\frac{t_{i,m}^3}{t_{i,m} + 2}\right). \quad (4d)$$

If a peak is clearly separated from its neighbours, then $T_{i,m}$ and $j_{i,m}$ are given directly. An estimate for t_i is more difficult to obtain because it requires a knowledge of the "apparent" activation energy E_i. The best way to proceed is to determine a series of estimates of E_i by several approaches.

The initial rise method [39], giving:

$$E_i \simeq -k \frac{d \ln j_i(T)}{d(1/T)} \quad (5)$$

may be applied when the low temperature tail of the ith peak is well developed. When it is possible to determine half widths, one may apply either Grossweiner's method [40]:

$$E_i \simeq \frac{1.51 kT_{i,m} T_{i,1/2}}{T_{i,m} - T_{i,1/2}} \quad (5a)$$

where $T_{i,1/2}$ the lower half-width temperature, or Van Turnhout's numerical approximations (Equation 3):

$$\frac{kT_{i,m}}{E_i} \simeq 0.69117 h_1 + 0.9088 h_1^2 + 2.1414 h_1^3 \quad (6)$$

where

$$h_1 = 1 - (T_{i,1/2}/T_{i,m}),$$

$$\frac{kT_{i,m}}{E_i} \simeq 1.0511\,h_2 + 0.18182\,h_2^2 \qquad (6a)$$

where

$$h_2 = -1 + (T^*_{1,1/2}/T_{i,m}),$$

and

$T^*_{i,1/2}$ is the upper half-width temperature.

The most reliable estimate for the apparent activation energy can be obtained by means of Bucci, Fieschi and Guidi's (BFG) [41] method, giving E_i by the slope of the line obtained when the logarithm of the remaining charge $Q_{i,r}(T)$ divided by the current $j_i(T)$ is plotted against T^{-1}. $Q_{i,r}(T)$ is given by a numerical computer evaluation of the integral $1/\beta \int_T^\infty j_i\,(T)\mathrm{d}T$. As an example, various E_i estimates have been derived for the prominent peak occurring in Fig. 2a and are compared in Table II. It is obvious that a good estimate for E_i falls somewhere between 0.4 and 0.5 eV.

TABLE II Estimates for E_i

Method	E_i (eV)
Initial rise	0.33
BFG	0.44
Half widths	
Grossweiner	0.5
Van Turnhout h_1	0.47
Van Turnhout h_2	0.4

When one of the components of the spectrum has been reconstructed, it is possible to determine starting values for the parameters of the other components by trial and error. All the estimated parameter values serve as initial values for a non-linear least-squares method* used to fit Equations 4a to the experimental values. Instead of the direct experimental values, their logarithms have been fitted to $\log [j_{tot}(T)]$, to avoid too slow convergence and underflow risks.

7. Discussion

The results of the TSD spectrum analysis by computer fit for the complete dose range are summarized in Table III. The fitted components and their algebraic sum are shown superimposed on the experimental points in Figs. 2a to h. The BR2 irradiation data are shown on an enlarged scale. The dependence on irradiation dose of the individual contributions are shown in Fig. 4. The reliability of the computer fit is relatively high. It has been tested by using different initial values and changing accuracy requirements. Yet, the final parameter values are subject to several error sources, mainly due to ill-defined starting values. These are caused either by the existence of relaxation peaks which are almost submerged between their neighbours or by the fact that one is too near the measured extremes of the spectrum. The lower temperature tail is disturbed by the fact that the heating rate requires some time to become constant. The higher temperature tail is difficult to determine, because it has to be cut off rather arbitrarily from the Maxwell–Wagner region, which shows a much higher current level (at least an order of magnitude larger). From Figs. 3 and 4 and Table III, one may observe that, aside from some deviations due to experimental scatter, a continuous line may be drawn between ^{60}Co and BR2 results.

The general conclusions which can be drawn from the given experimental results are the decreasing relaxation strength and the growing complexity of the spectrum with increasing dose. The number of components required for describing the spectrum goes from 3 for the as-received material to 4 between 20 and 100 Mrad and even to 5 above 200 Mrad. The given dose ranges, in which new effects appear, are not unambiguously determined, due to the fact that the "new" peaks may be present at lower dose, but hidden under the strongly dominant central peak. To illustrate the complexity of the spectrum at high doses, Fig. 5 shows a 400 Mrad spectrum, recorded in conditions, somewhat different from those mentioned in Table I (here $E_p = 250\,\mathrm{kV\,cm^{-1}}$, $t_p = 90$ min). The central peak (~218 K) is enclosed between two sharp peaks which appear to be generated by irradiation.

The parameters resulting from the computer fit $(E_i, T_{i,m}, j_{i,m})$ have reproducible values within the whole dose range. Problems may arise in those regions, where "new" peaks appear (~10 Mrad, ~200 Mrad), which are not well developed, resulting in a discrepancy in parameter values. As seen from Equations 4a, errors on the fitted parameter values accumulate in $\tau_{0,i}$, often leading to strongly deviating values for $\tau_{0,i}$. Nevertheless, when due

* The non-linear least squares method "FATAL" [42] is a part of the standard library of the S.C.K./C.E.N. IBM 370/135 Computer.

TABLE III Analysis of post-irradiation TSD spectra (part I–^{60}Co irradiated)

Dose (Mrad)	Component no.	Activation enthalpy (eV)	$\tau_{0,i}$ (sec)	Peak temperature T_m(K)	Relaxation strength (reduced units 10^{-7} m^2 sec^{-1})
0	1	0.20 ± 0.02	5×10^{-5}	183 ± 1	0.90 ± 0.05
	2	absent	–	–	–
	3	0.45 ± 0.01	4×10^{-8}	222 ± 0.5	7.8 ± 0.12
	4	absent	–	–	–
	5	0.52 ± 0.02	2×10^{-8}	249 ± 1	2.81 ± 0.04
5	1	0.31 ± 0.05	1×10^{-5}	199 ± 7	0.8 ± 0.1
	2	absent	–	–	–
	3	0.55 ± 0.05	2×10^{-8}	228 ± 1	6.1 ± 0.3
	4	absent	–	–	–
	5	0.52 ± 0.02	4×10^{-8}	256 ± 1	3.4 ± 0.1
10	1	0.23 ± 0.02	1.1×10^{-3}	195 ± 1	0.82 ± 0.06
	2	absent	–	–	–
	3	0.49 ± 0.04	1.4×10^{-7}	224 ± 1	4.0 ± 0.1
	4	1.0 ± 0.1	1.3×10^{-19}	239 ± 1	1.7 ± 0.3
	5	0.71 ± 0.05	2.6×10^{-12}	251 ± 1	2.5 ± 0.4
20	1	0.19 ± 0.07	1.5×10^{-2}	195 ± 8	0.8 ± 0.2
	2	absent	–	–	–
	3	0.5 ± 0.1	1.6×10^{-9}	219 ± 2	3.4 ± 0.8
	4	0.94 ± 0.1	1.2×10^{-18}	232 ± 3	1.4 ± 0.5
	5	0.60 ± 0.05	1.7×10^{-10}	243 ± 1	2.6 ± 0.4
50	1	0.21 ± 0.03	5×10^{-3}	197 ± 0.5	1.3 ± 0.2
	2	absent	–	–	–
	3	0.6 ± 0.1	1.4×10^{-11}	224 ± 1	3.6 ± 0.6
	4	1.1 ± 0.1	5.2×10^{-22}	234 ± 1	1.4 ± 0.2
	5	0.54 ± 0.12	2×10^{-12}	254 ± 1	2.4 ± 0.2
100	1	0.20 ± 0.02	5×10^{-4}	193 ± 2	1.1 ± 0.1
	2	absent	–	–	–
	3	0.5 ± 0.1	1.6×10^{-9}	219 ± 3	2.5 ± 0.5
	4	1 ± 0.1	4.2×10^{-20}	231 ± 3	1.5 ± 0.5
	5	0.54 ± 0.02	1.5×10^{-10}	246 ± 1	2.5 ± 0.2

account is taken of this possibility of extra large errors in τ_o, it appears that the τ_o values fall in three ranges: about 10^{-3} sec for process 1, about 10^{-9} sec for processes 3 and 5, and about 10^{-19} sec for processes 2 and 4.

We next discuss separately the parameters of the different components in relation to the molecular processes responsible for the relaxations.

Component 1: apparent activation energy, ~0.2 eV; peak temperature, ~190 K. As discussed already, the shape and width of this component cannot always be well determined, since this peak occurs too near the lower limit of the available temperature range. The relaxation strength slowly decreases from 1.2×10^{-7} red. units* at zero dose to 0.5×10^{-7} red. units at 400 Mrad, and can in first approximation be treated as a constant. This peak is usually attributed to the γ-relaxation phenomenon in PVDF [11]. As only small (2 to 4 monomer units), isolated segments [10] of the chain backbone are involved in the dipolar rotation, the relaxation strength is hardly depressed by the radiation cross-linking, in agreement with the experimental results. The low $\tau_{0,1}$ value can probably be explained by the difference between the apparent activation energy used in the analysis of the TSD experiments (0.2 eV) and the true activation energy (≈0.5 eV [11]).

Component 2: apparent activation energy, ~0.9 to 1.eV; peak temperature, ~207 K. this sharp peak is only detectable in the dose range corresponding to the BR2 irradiation. It will be

* red. units = reduced units (see third paragraph, Section 6)

TABLE III Decomposition of post-irradiation spectra (part II – "BR2" irradiated)

Dose (Mrad)	Component no.	Activation enthalpy (eV)	$\tau_{0,i}$ (sec)	Peak temperature T_m(K)	Relax. strength (reduced units 10^{-7} m^2 sec^{-1})
100	1	0.18 ± 0.02	5×10^{-2}	203 ± 10	0.6 ± 0.3
	2	absent	–	–	–
	3	0.34 ± 0.08	1.1×10^{-5}	218 ± 6	1.3 ± 0.3
	4	0.7 ± 0.5	5.7×10^{-11}	233 ± 5	0.7 ± 0.3
	5	0.43 ± 0.03	2.6×10^{-6}	245 ± 2	1.7 ± 0.1
200	1	0.22 ± 0.01	2.5×10^{-3}	186 ± 1	0.56 ± 0.02
	2	0.9 ± 0.3	3×10^{-20}	207 ± 1	0.10 ± 0.02
	3	0.40 ± 0.02	2.4×10^{-7}	214 ± 0.5	1.08 ± 0.03
	4	0.7 ± 0.1	2.5×10^{-13}	232 ± 0.5	0.81 ± 0.04
	5	0.54 ± 0.01	5.4×10^{-9}	246.2 ± 0.1	1.33 ± 0.01
300	1	0.18 ± 0.02	2.9×10^{-2}	195 ± 2	0.65 ± 0.05
	2	0.9 ± 0.05	3.6×10^{-20}	207.7 ± 0.7	0.3 ± 0.1
	3	0.58 ± 0.06	2.5×10^{-11}	217 ± 1	0.7 ± 0.1
	4	0.7 ± 0.2	4.6×10^{-13}	233.5 ± 0.5	0.5 ± 0.1
	5	0.42 ± 0.02	5.2×10^{-6}	247 ± 1	1.45 ± 0.05
400	1	0.40 ± 0.04	2×10^{-8}	194 ± 1	0.38 ± 0.08
	2	1.0 ± 0.05	7.4×10^{-23}	200 ± 1	0.14 ± 0.03
	3	0.40 ± 0.04	2.4×10^{-7}	214 ± 1	0.81 ± 0.08
	4	0.9 ± 0.1	1×10^{-17}	233.3 ± 0.7	0.66 ± 0.08
	5	0.56 ± 0.02	2.5×10^{-9}	248.0 ± 0.6	1.20 ± 0.04

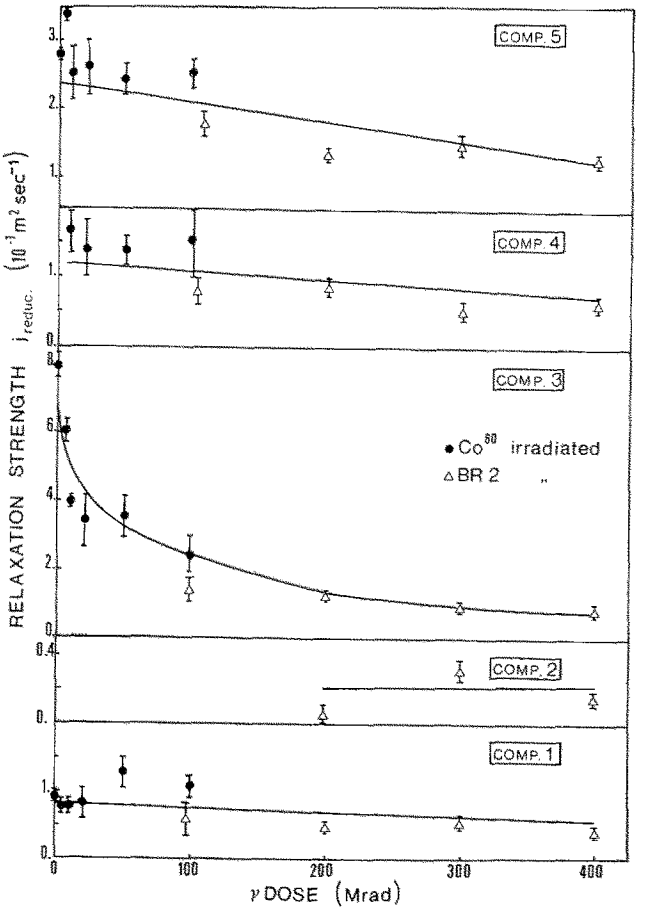

Figure 4 Dependence on γ dose of the relaxation strength of the TSD components resulting from the computer fit.

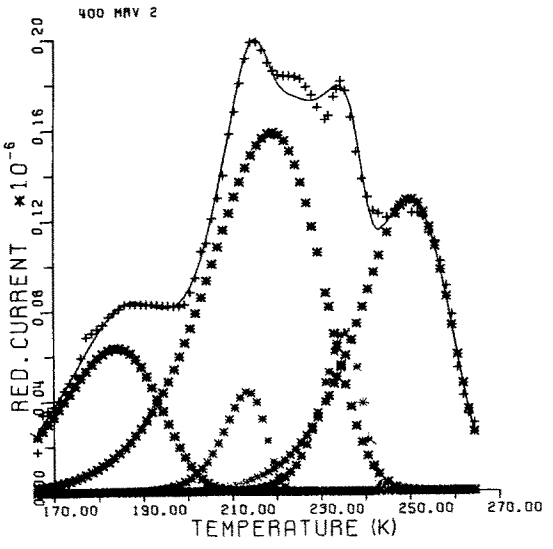

Figure 5 Plot illustrating the complexity of TSD spectra at higher irradiation doses. This plot has been recorded for conditions somewhat different from those for Fig. 2a to h ($E_p = 250\,kV\,cm^{-1}$, $t_p = 90$ min).

discussed together with component 4, which appears to have comparable characteristics.

Component 3: apparent activation energy, ~0.5 eV; peak temperature, ~220 K. This component is the main cause of the strong depression of the total relaxation strength of the region below room temperature (Fig. 4). The main fall-off (~50%), occurs at early stages of irradiation, i.e. during the sharp increase in cross-linking (see Section 3); it continues slowly up to heavy doses (100 to 400 Mrad). Taking account of its zero dose position (~225 K), this component may be related to the β-relaxation or glass transition T_g [11], corresponding to the micro-Brownian motion of the main chain backbone. Although a large scatter exists, one may observe a decrease of the peak temperature with increasing dose (Fig. 6), not observable by DTA experiments in this temperature region. The peak temperature shift may be attributed to loss of crystallinity rather than to cross-linking. Boyer [10] points out that T_g is usually pushed down a few degrees with decreasing degree of crystallinity. However, no quantitative relationship has been developed between χ and T_g.

Considering the specific properties of the glass transition, it is possible to relate them to the depression in peak intensity. It has been suggested by Boyer [10] that for the glass transition of semi-crystalline polymers chain segments of at least 25 to 50 co-operating monomer units are necessary. Through the creation of anchoring points by radiation cross-linking, the number of such chain segments is reduced and hence (Equation 4a″) corresponding TSD relaxation strength. The fraction α_R of monomer units taking part in the relaxation, can thus be estimated from the TSD peak intensity: $\alpha_R = N_D/N_T$.

$$N_D = \frac{3kT_{3,m}Q}{A\mu_i^2 E_p} \tag{7}$$

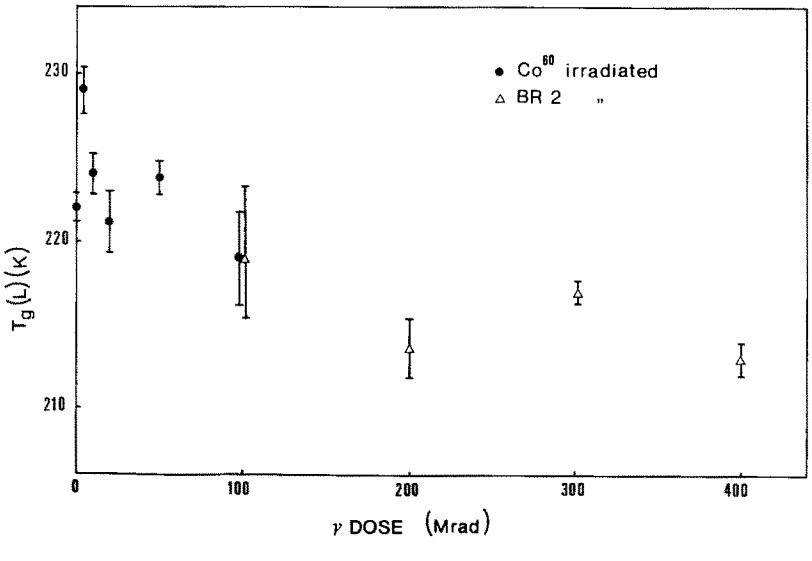

Figure 6 Dose dependence of $T_g(L)$, the peak temperature of component 3, corresponding to the β relaxation or glass transition.

is the number of monomer units which take part in the reorientation [44]:

$$N_T = \rho \frac{N_A}{M}(1-\chi) \qquad (7')$$

is the total number of monomer units in the amorphous phase. A is the electrode area, Q the charge released during the reorientation (evaluated either numerically by computer integration or graphically from the TSD peak area), ρ the density, N_A Avogadro's number and M the monomer molecular weight. Hence;

$$\alpha_R = \frac{3kMT_{3,m}Q}{\rho A \mu_i^2 E_p N_A (1-\chi)} \equiv K\frac{QT_{3,m}}{(1-\chi)}. \qquad (8)$$

K contains the dose-independent factors. $Q, T_{3,m}$, χ and α_R are given in Table IV. χ has been evaluated from the decrease in crystalline melting temperature, as obtained from DTA experiments (Flory's Equation 22, see Section 3). μ_i has been estimated $\simeq 2$ Debye from a simple summation of the monomer dipole moments [45]. The resulting α_R values appear reasonable. The zero dose value is less than one, due to the existence of several mobility reducing defects in the unirradiated material (cross-links, chain-ends, side-branches, etc).

These α_R values may now be compared with the fractions, calculated from molecular length distributions as changed by irradiation cross-linking. Indeed, the probability that chain segments longer than a critical molecular length occur, will decrease, when the available molecular length between cross-linking points is reduced [46]. Considering the simple case of a Schulz–Zimm-like molecular length distribution of the *0th* degree for the unirradiated material, Kimura [47] has derived a distribution $w(p)$ for the molecular lengths p between cross-links:

$$w(p) = \frac{1}{u^2}\exp\left[-\frac{p}{u}(2ut+1)\right] \equiv \frac{1}{u^2}\exp(-v) \qquad (9)$$

where $u = M_n/M$ is the number average degree of polymerization, (M_n is the number average molecular weight) and $t = CR$, C being the cross-linking probability and R the dose. C is related to the yield value for cross-linking $G(C)$ by [48]:

$$G(C) \simeq 0.97 \times 10^6 \frac{C}{M}.$$

TABLE IV

Dose (Mrad)	$T_{3,m}$(K)	χ	$Q \times 10^8$(C)	α_R
0	222	0.44	11	0.85
5	228	0.43	8.3	0.66
10	224	0.43	5.3	0.41
20	219	0.42	4.8	0.35
50	224	0.41	4	0.29
100	218	0.40	2.8	0.20
200	214	0.35	2.2	0.14
300	217	0.31	1.84	0.11
400	214	0.28	1.32	0.08

$G(C)$ may be evaluated from the Charlesby–Pinner relation of insoluble fraction and dose.

Putting $v_o = p_o\,(2ut+1)/u$ one can easily predict the fraction α_p ($p \geqslant p_0$) of molecular lengths larger than a critical length p_o:

$$\alpha_p(p \geqslant p_0) = \int_{v_o}^{\infty} e^{-v}dv \Big/ \int_{o}^{\infty} e^{-v}dv = e^{-v_o}. \qquad (9a)$$

Inversely, knowing a certain fraction, it should be possible to estimate p_o when using a suitable fitting method. To account for the zero-dose effects, making α_R non-unity, a correction term C_o should be included in t: $t = CR + C_o$. p_o and C_o now serve as parameters in the computer fit by Equation (9a). The numerical factors C and u have been estimated by [31]: $G(C) \simeq 2$, giving $C \simeq 1.3 \times 10^{-4}$ (Mrad)$^{-1}$ and [43]: $u = M_n/M = 4 \times 10^4/64 = 625$. Fitting results are summarized in Table V and Fig. 7. Equation (9a) does not cover the entire range of α_R values. Attributing weight one to every α_R value leads to a good fit for the steep initial decrease yielding a somewhat too high p_o value and an acceptable C_o value. Attributing $(\alpha_R)^{-1}$ weights leads to a good fit for the tail values, leading to a good p_o value and a too high C_o value. Fitting with higher order Schulz–Zimm initial distributions does not yield better fitting results. Therefore, it is thought that Equation (9′) might result

TABLE V Fitting results for α_R fitted by a molecular length distribution

Parameters resulting from fit	Weights taken $(\alpha_R)^{-1}$	Weights taken 1
$\bar{p}_o$	25 ± 7	78 ± 20
C_o	(1.3 ± .6) 10^{-2}	(1.5 ± 1) 10^{-3}
Curve in Fig. 7	1	2

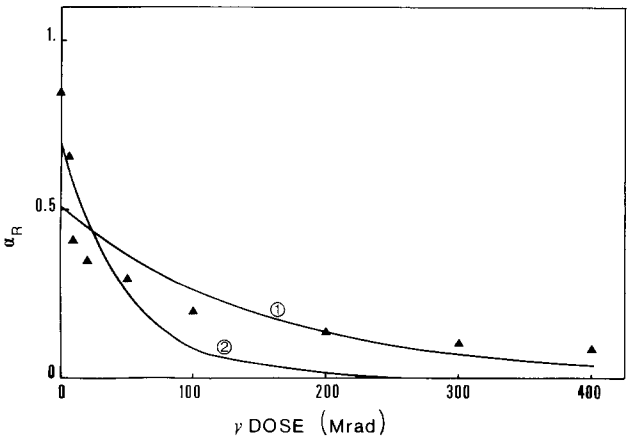

Figure 7 Dependence on γ dose of α_R, the fraction of the total number of monomer units taking part in the β reorientation process. Superimposed are the results of the computer fits by Equation 9a of which the parameters are listed in Table V.

in an acceptable description provided it is corrected for the following points:

(1) the effect of saturation cross-linking which has been observed experimentally (Section 3.) should be included;

(2) C_0 should be determined in terms of fundamental molecular data;

(3) the density of experimental data points in the low dose range should be increased.

Component 4: apparent activation energy, 0.7 to 1 eV; peak temperature, 232 K. This depolarization peak presents some features which are very reminescent of component 2. Both peaks appear upon γ-iradiation, component 4 at 10 Mrad, component 2 at 200 Mrad. Since they are reproducible during subsequent TSD measurements, they cannot be interpreted as being caused by detrapping of charge carriers, but they appear to be due to genuine dipolar structural defects. The common feature of both peaks is their sharpness, which is probably related to their high apparent activation energy and the corresponding very low τ_0 value compared to the neighbouring peaks (cf. Table III).

A number of apparently similar effects reported in the literature have been attributed to a number of different causes. Perlman *et al.* [9] found a sharp increase of some peaks in their thermally stimulated current (TSC) spectra of corona-charged polyethylene and PTFE, which they attribute to trapping at the created double bonds, whereas Hedvig [49] attributes TSD peak doubling in the polyethylene glass transition region to the existence of two amorphous phases in the material. Kreahling and Kline [50], on the other hand, have invoked the irradiation-induced creation of double trans-polyene groups (—C=C—C=C—. . .—) performing a "crankshaft"-type of motion to explain "new" internal friction peaks in γ-irradiated PVC. Pursuing this last line of reasoning, it appears plausible to relate our new TSD peaks in PVDF to the generation of polyenyl-radical groups. Indeed, Seguchi *et al.* [51] have shown that at room temperature, the fluorinated polyenyl radical $-(-CF=CH-)_n-\dot{C}F$ may be stable. This is confirmed by the production of large quantities of HF (yield factor for HF formation about 3 [48]), following the reactions:

$$-CH_2-\dot{C}F-CH_2 \xrightarrow{-HF} \ldots -CH_2-CF=CH-\dot{C}F-\ldots$$

$$\xrightarrow{-HF} \ldots -CH_2-(CF=CH)_2-\dot{C}F-\ldots$$

$$\xrightarrow{-HF} \ldots -CH_2-(CF=CH)_n-\dot{C}F-\ldots$$

Further evidence for polyenyl formation comes from post-irradiation infra-red spectra (Section 3). The increase with dose of the intensity of the absorption bands in the range of 1600 to 1900 cm^{-1} is attributed to the increasing number of double bonds. There are good reasons to believe that polyene chain segments may effect dipolar reorientations. Therefore, we suggest the possibility that the "new" peaks in the case of PVDF are due respectively to a local mode vibration and to a main glass transition, but not for polyene chain segments.

Component 5: apparent activation energy, about 0.5 eV; peak temperature, ~ 250 K. As already mentioned, the shape of the 5th component is difficult to define, because one has to decide rather arbitrarily the cut-off from the Maxwell–Wagner region. It is therefore surprising that as a result of the computer fit, such narrow limits for the apparent activation energy have been found. The relaxation strength of the 5th component

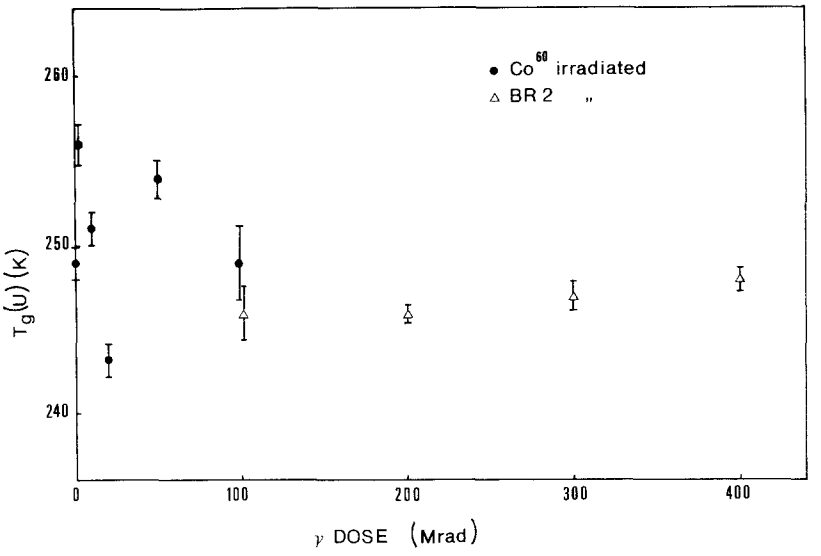

Figure 8 Dose dependence of $T_g(U)$, the peak temperature of component 5, probably corresponding to the upper glass transition.

decays only very slowly with γ dose. Although there is a lot of scatter, there is some indication for a slight decrease in peak temperature (Fig. 8).

This depolarization peak probably corresponds to the one observed at -10° C by Takamatsu *et al.* [13].

Several experimental facts about this peak have led the present authors to the supposition that it may be related to what Boyer [10] calls "the apparent upper glass transition", $T_g(U)$. Boyer assumes that the chains in an amorphous material, which is put under restraint by the presence of crystallites, may perform hindered rotation-like motions about the chain backbone. He therefore expects $T_g(U)$ at a somewhat higher temperature than the main glass transition $T_g(L)$, which occurs in material free of restraints.

Boyer [10] mentions a few experimental data, which can be interpreted in terms of the presence of this upper glass transition and suggests the amorphous material in the interlamellar disorganized chains to be responsible for it.

Our material meets the requirements for a TSD detection of $T_g(U)$, as they have been proposed by Boyer: $T_g(L)$ and the crystalline melting temperature T_{CM} are indeed separated sufficiently from each other and the degree of crystallinity is about 50%. The characteristics of the *5th* component, as derived from the computer fit, also strongly support the above supposition:

(a) the activation energy (0.5 eV) is comparable to the $T_g(L)$ apparent activation energy (see component 3);

(b) $T_g(U)$ decreases slowly with dose (Fig. 8). This can be due to the depression of the degree of crystallinity, reducing the number of crystallites. $T_g(U)$ appears less affected by the low-dose cross-linking, because, as Boyer points out, shorter chain segments than for $T_g(L)$ are involved. Hence, hindering is less effective;

(c) the peak intensity also decreases slowly with dose, and this may be explained by the same argument as used for (b);

(d) The present TSD peak can be fitted into the Arrhenius plot for $T_g(u)$, as it was composed by Boyer, taking the equivalent frequency as $(1. \pm 0.4)$ 10^{-4} Hz, based on a calculation suggested in [3]. The corresponding (real) activation energy is ~ 1.2 eV.

8. Conclusions

Thermally stimulated depolarization has been used to study the post-irradiation behaviour of the semi-crystalline polymer PVDF. Because of its large resolving power, it was possible to distinguish five relaxation peaks in the TSD spectra below room temperature. The dependence of the relaxation strengths and peak temperatures of these peaks has been used for identifying the underlying processes at the molecular level:

(1) component 1 (0.2 eV, $T_p \sim 190$ K), corresponds to the γ relaxation, a local mode process

which is not strongly disturbed by the irradiation;

(2) components 2 and 4 (~1 eV, $T_p \sim 207$ and 232 K respectively) are probably a radiation effect. A speculative interpretation attributes them to rotational processes of polyene chain segments, created by irradiation;

(3) component 3 (~0.5 eV, $T_p \sim 220$ K) corresponds to the β relaxation, which is related to the glass transition. It is the main cause for the strong depression of the relaxation strength below room temperature. This decrease in relaxation strength is due to a reduction of the chain mobility by irradiation cross-linking;

(4) component 5 (~0.5 eV, $T_p \sim 250$ K) is probably the depolarization effect accompanying the apparent upper glass-transition $T_g(U)$.

Acknowledgements

The authors wish to thank the Research Division of Solvay, especially Dr Majot, for their kindness in supplying the specimens. They also thank Mr Gandolfo and Mr Boeykens (BR2) for the irradiations, Mr Van Springel (RUCA) for the infra-red experiments and Mr Schreynemaeckers (RUCA) for the X-ray measurements. The authors are indebted to Dr Nagels and Dr Nihoul for their critical reading of the manuscript.

References

1. B. GROSS, "Charge storage in solid dielectrics" (Elsevier, Amsterdam, 1964).
2. M. M. PERLMAN, *J. Electrochem. Soc.* **119** (1972) 892.
3. J. VAN TURNHOUT, "Thermally stimulated discharge of polymer electrets" (Elsevier, Amsterdam, 1975).
4. H. J. WINTLE, *J. Acoust. Soc. Amer.* **53** (1973) 1578.
5. P. HEDVIG and A. SOMOGYI, "Proceedings of the 3rd Tihany symposium on Radiation chemistry", Edited by J. DOBO and P. HEDVIG (Akadémiai Kiadó, Budapest, 1972) p. 907.
6. KH. SOLUNOV and P. HEDVIG, *ibid* p.899.
7. A. E. BLAKE, A. CHARLESBY and K. J. RANDLE, *J. Phys. D: Appl. Phys.* 7 (1974) 760.
8. M. GRINTEN and C. BOULT, *ibid* 8 (1975) L159.
9. M. M. PERLMAN and S. UNGER, *ibid* 5 (1972) 2115.
10. R. F. BOYER, *J. Polymer Sc., Symp.* **50** (1975) 189.
11. A. CALLENS, R. DE BATIST and L. EERSELS, *Nuovo Cimento* **33B**, (1976) 434.
12. R. A. CRESWELL, M. M. PERLMAN and M. A. KABAYAMA in "Dielectric Properties of Polymers", edited by F. E. KARASZ (Plenum Press, New York, 1972).
13. T. TAKAMATSU and E. FUKADA, *Polymer J.* **1** (1970) 101.
14. G. PFISTER and M. A. ABKOWITZ, *J. Appl. Phys.* **45** (1974) 1001.
15. M. ABKOWITZ and G. PFISTER, *ibid* **46** (1975) 2559.
16. G. PFISTER, M. ABKOWITZ and R. G. CRYSTAL, *J. Appl. Phys.* **44** (1973) 2064.
17. H. BURKARD and G. PFISTER, *ibid* **45** (1974) 3360.
18. M. TAMURA, K. OGASAWARA, N. ONO and S. HAGIWARA, *ibid* **45** (1974) 3768.
19. A. I. BAISE, H. LEE, B. OH, R. E. SALOMON and M. M. LABES, *Appl. Phys. Letters* **26** (1975) 428.
20. Y. GAL'PERIN, B. KOSMYNIN and V. SMIRNOV, *Vysokomol. Soyed* **A12** (1970) 1880.
21. T. SUWA, T. SEGUCHI, K. MAKUUCHI, T. ABE, N. TAMURA and M. TAKEHISA, *Rep Prog. Polymer Phys. Japan*, **XV** (1972) 503.
22. P. J. FLORY, *J. Chem. Phys.* **15** (1947) 684.
23. R. P. KUSY and D. T. TURNER, *Rad. Chem.* **4B** (1971) 337.
24. T. SUWA, T. SEGUCHI, K. MAKUUCHI, T. ABE, N. TAMURA and M. TAKEHISA, *J. Chem. Soc. Japan, Chem. Ind. Chem.* **5** (1973) 1046.
25. J. K. BROWN and K. J. MORGAN in "Advances in fluorine chemistry", Vol. 4 (Butterworths, London, 1965) p. 253.
26. N. B. COLTHUP, L. H. DALY and S. E. WIBERLEY, "Introduction to Infra-red and Raman Spectroscopy" (Academic Press, New York, 1975) p. 251.
27. N. L. ALPERT, W. E. KEIZER and H. A. SZYMANSKI, "I.R. Theory and practice of infrared spectroscopy" (Plenum Press, New York, 1970) pp. 283, 252.
28. K. MAKUUCHI, T. SEGUCHI, T. SUWA, T. ABE, N. TAMURA and M. TAKEHISA, *Rep. Prog. Polymer Phys. Japan* **XV** (1972) 499.
29. A. CHAPIRO, "Radiation chemistry of polymeric systems" (Interscience, New York 1962) p. 385.
30. G. D. SANDS and G. F. PEZDIRTZ, *Polymer Preprints* **6** (1965) 987.
31. T. YOSHIDA, R. E. FLORIN and L. A. WALL, *J. Polymer Sci.* **A3** (1965) 1685.
32. A. R. VON HIPPEL, "Dielectrics and waves" (Wiley, New York, 1954).
33. V. V. DANIEL, "Dielectric relaxation" (Academic Press, London, 1967).
34. T. J. GRAY, Office of Naval Research, Project N–015215 (1965).
35. A. CALLENS, unpublished results.
36. V. K. MATVEEV, S. E. VAISBERG and V. L. KARPOV, *Sov. Plastics* **9** (1971) 48.
37. T. COWELL and J. WOODS, *Brit. J. Appl. Phys.* **18** (1967) 1045.
38. P. C. MEHENDRU, K. JAIN, V. K. CHOPRA and PRAVEEN MEHENDRU, *J. Phys. D. Appl. Phys.* **8** (1975) 305.
39. G. F. GARLICK and A. F. GIBSON, *Proc. Roy. Soc.* **60** (1948) 574.
40. R. I. GROSSWEINER, *J. Appl. Phys.* **24** (1953) 1306.
41. C. BUCCI, R. FIESCHI and G. GUIDI, *Phys. Rev.* **148** (1966) 816.
42. L. SALMON and D. V. BOOKER, "Subroutine

FATAL", AERE-R7129 (1972).
43. Unpublished data of Solvay Research Center, Brussels.
44. R. A. CRESWELL and M. M. PERLMAN, *J. Appl. Phys.* **41** (1970) 2365.
45. S. YANO, *J. Polymer Sci. A-2* 8 (1966) 1057.
46. O. SAITO, "The radiation chemistry of macromolecules", Vol. 1, edited by M. DOLE (Academic Press, New York, 1972) Ch. 11, p. 223.
47. T. KIMURA, *J. Phys. Soc. Japan* **17** (1962) 1884.
48. K. MAKUUCHI, T. SEGUCHI, T. SUWA, T. ABE, N. TAMURA and M. TAKEHISA, *Nippon, Kagaku Kaishi,* 8 (1973) 1574.
49. P. HEDVIG, "Kémiai Közlemények" (MTA, Budapest, 1971).
50. R. P. KREAHLING and D. E. KLINE, *Kolloid Z.uZ. Polymere* **206** (1965) 1.
51. T. SEGUCHI, K. MAKUUCHI, T. SUWA, N. TAMURA, T. ABE and M. TAKEHISA, *Rep. prog. Polymer Phys. Japan* **XV** (1972) 513.

Received 11 October and accepted 22 November 1976.